

Millimeter-Wave Integrated-Horn Antennas: Part II—Experiment

Walid Y. Ali-Ahmad, *Student Member, IEEE*, George V. Eleftheriades, *Student Member, IEEE*,
Linda P. B. Katehi, *Senior Member, IEEE*, and Gabriel M. Rebeiz, *Member, IEEE*

Abstract—The impedance and radiation patterns of a dipole-fed integrated horn antenna in a ground plane are experimentally investigated at microwave and millimeter-wave frequencies. The agreement with the full-wave analysis technique presented in Part I is good. The results indicate that for a 70° flare-angle horn, horn apertures from 1.0λ -square to 1.5λ -square with dipole positions between 0.36 and 0.55λ yield good radiation patterns with a gain between 10 – 13 dB, a cross-polarization level lower than -20 dB, and resonant dipole impedances between 40Ω and 120Ω . It is also found that the impedance measurements can be safely used for two-dimensional horn arrays, but the radiation patterns differ because of the Floquet modes associated with the array environment. The integrated horn antenna is a high-efficiency antenna suitable for applications in millimeter-wave imaging systems, remote-sensing, and radio astronomy.

I. INTRODUCTION

THIS is the second of two papers on the analysis and measurements of a dipole-fed integrated-horn antenna in a ground plane (Fig. 1). The first paper [1] presented a full-wave analysis technique for the calculation of the input impedance of the feeding dipole and the radiation patterns of the horn antennas. The convergence properties of the method were investigated, along with the resonant properties of the strip-dipole and the corresponding behavior of the far-field patterns. In this paper, the design of an integrated-horn antenna with a flare-angle of 70° is presented and microwave and millimeter-wave impedance and pattern measurements are compared with theory. The paper concludes with a comparison between an integrated-horn antenna in a ground plane and in a two-dimensional array.

II. INTEGRATED-HORN ANTENNA DESIGN

The integrated-horn antenna is fabricated using silicon-nitride membrane technology and anisotropic etching of silicon. The antenna is composed of a minimum of two stacked wafers. The thickness of the front wafer determines the position of the dipole antenna inside the horn cavity. The opening on the front wafer determines the aperture size of the horn. The back wafer acts as a reflecting cavity and completes the horn structure. The dipole antenna, detector, and

Manuscript received November 26, 1990; revised July 12, 1991. This work was supported by the NASA/Center for Space Terahertz Technology at the University of Michigan.

The authors are with the NASA/Center for Space Terahertz Technology and the Department of Electrical Engineering and Computer Science, The University of Michigan, Ann Arbor, MI 48109.
IEEE Log Number 9103276.

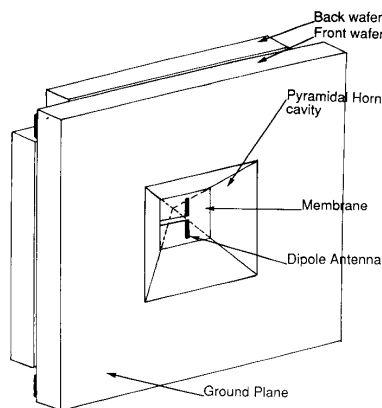


Fig. 1. A monolithic integrated horn antenna in a ground plane.

transmission lines are integrated on the back side of the front wafer. The dipole antenna is integrated on a $1 \mu\text{m}$ thin dielectric membrane and is effectively suspended in the horn cavity. The flare angle is fixed by the orientation of the crystal planes at 70.6° . Details of the fabrication procedure are presented in [2], [3].

The design of the horn antenna involves the selection of the horn aperture size and the dipole position in the cavity. A horn aperture smaller than 0.8λ results in a wide radiation pattern with a directivity around 8 dB. This pattern does not have any advantage over elementary antennas such as a dipole backed by a ground plane. On the other hand, a horn aperture greater than 1.7λ suffers from aperture phase errors due to the large flare angle of the horn [4]. Also, the horn radiation pattern and the dipole input impedance are strongly dependent on the dipole position inside the horn cavity. For example, a dipole position close to the apex lies near the cutoff region of the horn and has a low input impedance while the high-order modes triggered by a dipole close to the aperture distort the aperture field and yield a poor radiation pattern. From our theoretical analysis of Part I, we find that for a 70° flare angle, horn apertures from 1.0λ -square to 1.5λ -square with dipole positions between 0.36 and 0.55λ result in good radiation patterns and practical values of dipole impedances.

III. IMPEDANCE MEASUREMENTS

A microwave model at 1 – 2 GHz was constructed for impedance measurements. The dipole antenna was fed using a coaxial cable and a coplanar-strip transmission line shorted

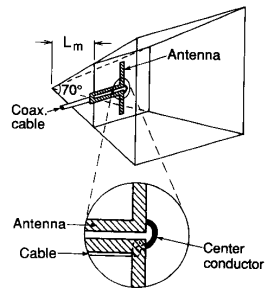


Fig. 2. Microwave impedance measurement setup at 1–2 GHz. The shorted coplanar-strips act as a balun and models the low-pass filter and the bias line in the 92 GHz antenna.

$\lambda/4$ away from the feed (Fig. 2). This design has two purposes. It models the low-frequency connection on the membrane effectively, and provides an effective balun for the coax-dipole transition. The dipole was also fed along the axis of the horn with a coaxial cable and an appropriate balun. Both measurements resulted in identical results.

The measured resonant resistance and resonant length of the feed dipole versus dipole position are compared with theory in Fig. 3. The resonant resistance is a strong function of the dipole position and varies from 25 to 175 Ω for dipole positions between 0.34 and 0.6 λ . The input impedances versus frequency for various feed positions are presented in Figs. 4 and 5. It is seen that the dipole impedance increases and becomes more wideband as the dipole is moved away from the apex. Also, as predicted by the full-wave analysis, the strip dipole cannot achieve resonance for feeding positions between 0.6 and 0.8 λ . There is a second region of resonance near the aperture of the horn, but the corresponding radiation patterns are poor. The impedance results therefore indicate that dipole positions between 0.36 and 0.55 λ should be used for Schottky diodes and SIS mixers.

IV. PATTERN MEASUREMENTS

An integrated horn antenna with an aperture of 1.35 λ -square and a dipole position of 0.38 λ from the apex was fabricated for microwave and millimeter-wave pattern measurements. The corresponding membrane is 0.54 λ -square. The dipole is placed at the center of the membrane, and a resistive bolometer detector is integrated at its apex. The 0.54 λ membrane allows the integration of a simple coplanar-strip $\lambda/4$ low-pass filter which results in a very large parallel impedance and the dipole apex [2]. The bolometer detector presents there a much lower impedance and absorbs all the received power.

A microwave model at 3 GHz with a ground-plane dimension of 2.5 λ -square was used for pattern measurements. For the 92 GHz measurements, the horn design resulted in a front and back wafer thicknesses of 1.9 and 1.25 mm, respectively. The front and back wafers were constructed from a stack of silicon wafers with nominal thicknesses of 760 and 380 μm (Fig. 6). The variation in wafer thickness and alignment repeatability introduced several 60 μm steps in the horn cavity. The horn sidewalls were gold coated except for a small portion near the dipole antenna. This reduces the

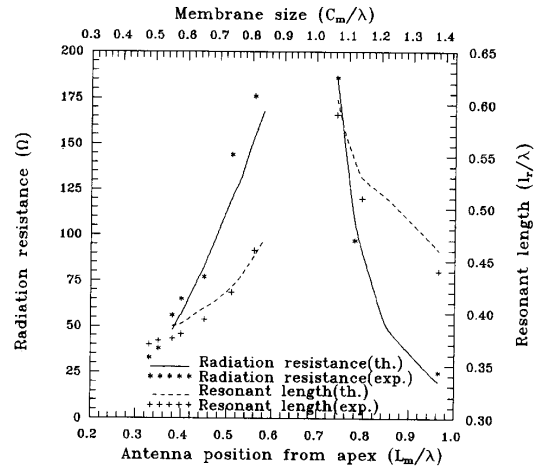


Fig. 3. Measured and predicted dipole resonant resistance and resonant length versus dipole position from the apex. Notice the region of no resonance in the center of the horn.

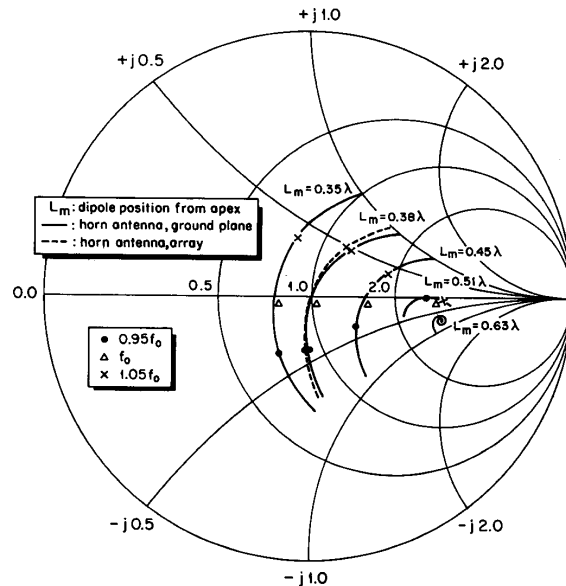


Fig. 4. The input impedances versus frequency for various feed positions in the horn cavity. The dipole input impedance increases and becomes more wideband as the dipole is moved away from the apex. The dashed line is the measured impedance of a dipole in a 3 \times 3 array.

efficiency of the horn antenna by approximately 0.3 dB and lowers the cross polarization by a 2–3 dB but has a negligible effect on the co-polarized pattern [2], [5]. The measured H -plane patterns (Figs. 7, 8) agree well with theory at 3 and 92 GHz. The discrepancy in the E -plane pattern for large angles are due to the finite size of the ground plane at 3 GHz, and to the steps in the sidewalls at 92 GHz. The cross-polarization component was not measurable in the E - and H -plane scans. The 45°-plane pattern also agrees well with

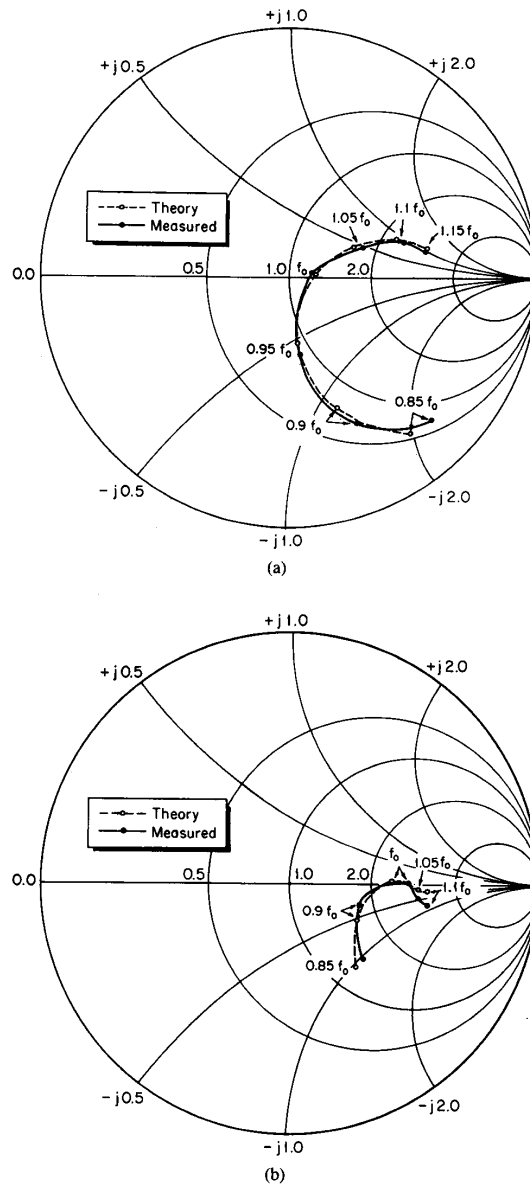


Fig. 5. Comparison between the measured and predicted dipole input impedance versus frequency for a feed position of 0.41λ (a) and 0.5λ (b).

theory (Fig. 8), but the cross-polarization component could not be measured due to signal-to-noise ratio limitations.

V. COMPARISON WITH TWO-DIMENSIONAL HORN ARRAYS

The measured input impedance for feed positions between 0.36 and 0.55λ did not change if the ground plane was removed or if the horn was placed in the middle of a 3×3 array. Also, for the dipole positions mentioned above, the measured (and predicted) impedance is insensitive to the horn aperture size. This is because at feed positions far from the

aperture, the impedance is determined mainly by the geometry of the horn cavity and not by the transition to free space. The predicted impedances and resonant lengths for a horn in an infinite ground plane can therefore be safely used for the design of two-dimensional horn arrays. Indeed, the experimentally determined resonant length and radiation resistance used by Guo *et al.* [5] for the design of an efficient 1λ imaging array agree well with our calculations and measurements for a 1.35λ horn in a ground plane with the same dipole position and dipole length (Fig. 4).

The patterns for a 1.35λ -square horn in a ground plane

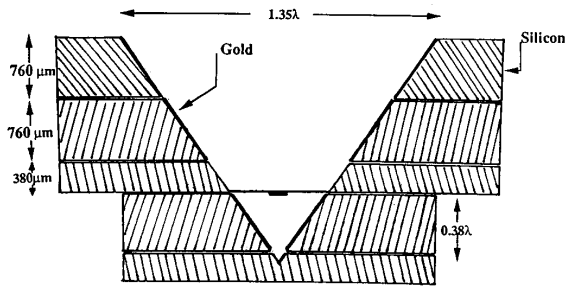


Fig. 6. The complete millimeter-wave antenna structure. Gold is not evaporated on the sidewalls of the 380 μm membrane wafer. The steps in the sidewalls between the wafers are around 60 μm and are due to variation in wafer thicknesses.

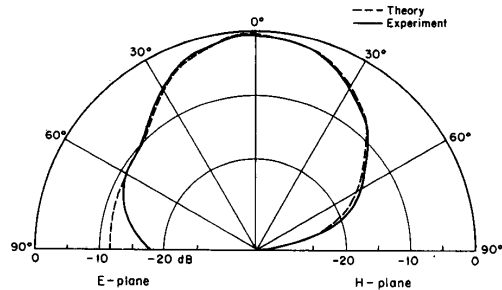


Fig. 7. Measured and predicted *E*- and *H*-plane patterns at 3 GHz. The discrepancies in the *E*-plane pattern at large angles is due to the finite size of the ground plane.

and in a two-dimensional array are shown in Fig. 9. Reciprocity and mode-matching technique at the horn aperture has been successfully used to predict the pattern of a horn element in a two-dimensional array [2]. The TE_{10} tapering of the electric field across the aperture yields a vanishing tangential electric field at the edges of the horn and therefore decouples the horn from the array environment. This results in an *H*-plane patterns that is similar to that of a horn in an infinite ground plane. In the case of the *E*-plane pattern, the horn sees the array and the spikes and nulls in the pattern are due to the discrete nature of the Floquet modes [6]. It is clear from the patterns that a horn in a two-dimensional array will always yield a higher gain and spillover efficiency than a horn in an infinite ground plane. This is due to the null in the *E*-plane pattern at 90° and is a result of the vanishing electric field at grazing angles in a two-dimensional array.

VII. CONCLUSION

A full theoretical and experimental characterization has been done on a 70° flare-angle integrated-horn antenna in a ground plane. The results indicate that horn apertures from 1.0 to 1.5 λ-square with dipole positions between 0.36 and 0.55 λ yield good radiation patterns and resonant dipole impedances between 40 and 120 Ω. Also, there exists a region inside the horn cavity with no possibility of dipole resonance. The impedance results can be safely extended to two-dimensional horn arrays, but the radiation patterns differ

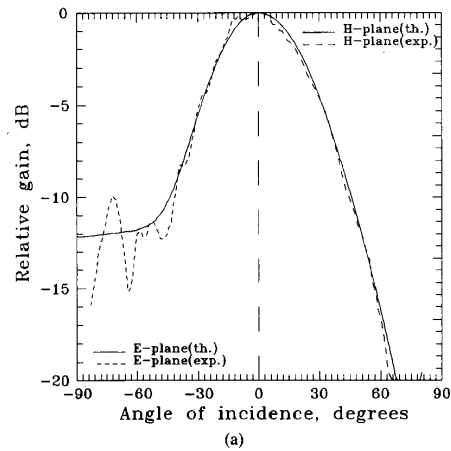


Fig. 8. Measured and predicted *E*, *H* (a) and 45°-plane (b) patterns at 92 GHz. The discrepancy in the *E*-plane pattern at large angles is due to the steps in the sidewalls. (Notice the different vertical scales on the 45° pattern graph.)

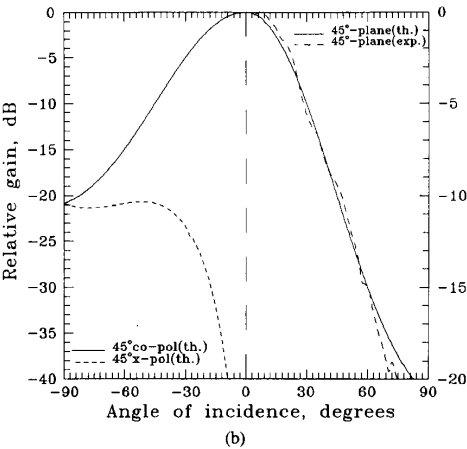


Fig. 9. The *E*- and *H*-plane patterns of a 1.35 λ horn antenna in a ground plane and in a two-dimensional array.

because of the Floquet modes associated with the array environment.

REFERENCES

- [1] G. V. Eleftheriades, W. Y. Ali-Ahmad, L. P. B. Katehi, and G. M. Rebeiz, "Millimeter-wave integrated-horn antennas: Part I—Theory," *IEEE Trans. Antennas Propagat.*, pp. 1575–1581, this issue.
 - [2] G. M. Rebeiz, D. P. Kasilingam, P. A. Stimson, Y. Guo, and D. B. Rutledge, "Monolithic millimeter-wave two-dimensional horn imaging arrays," *IEEE Trans. Antennas Propagat.*, vol. 38, pp. 1473–1482, Sept. 1990.
 - [3] G. M. Rebeiz, "Millimeter-wave two-dimensional horn imaging arrays," Ph.D. dissertation, California Inst. Technol., Pasadena, June 1988.
 - [4] C. A. Balanis, *Antennas: Theory and Design*. New York: Harper and Row, 1984.
 - [5] Y. Guo, K. Lee, P. A. Stimson, K. A. Potter, and D. B. Rutledge, "Aperture efficiency of integrated-circuit horn antennas," *Microwave Opt. Tech. Lett.*, vol. 4, no. 1, pp. 6–9, Jan. 1991.
 - [6] N. Amitay, V. Galindo, and C. P. Wu, *Theory and Analysis of Phased Array Antennas*. New York: Wiley, 1972.
- Walid Y. Ali-Ahmad** (S'89), for a photograph and biography please see page 825 of the June 1991 issue of this TRANSACTIONS.
- George V. Eleftheriades** (S'88), for a photograph and biography please see page 1581 of this issue.
- Linda P. B. Katehi** (S'81–M'84–SM'89), for a photograph and biography please see page 1045 of the July 1990 issue of this TRANSACTIONS.
- Gabriel M. Rebeiz** (S'86–M'88), for a biography please see page 825 of the June 1991 issue of this TRANSACTIONS.